sciendo

*Polish Journal of Chemical Technology, 20, **4**, 129—137, 10.2478/pjct-2018-0065*

Numerical investigation of the turbulent flow generated with a radial Turbine using a converging hollow blade

Mousaab Beloudane[1*], Mohamed Bouzit[1], Houari Ameur[2]

[1]Département de génie mécanique, Laboratoire des Sciences et Ingénierie Maritimes, Faculté de Génie Mécanique, Université des Sciences et de la Technologie Mohamed Boudiaf d'Oran, B.P. 1505 Oran, Algeria
[2]Institute of Science and Technology, University Center Ahmed Salhi, Ctr Univ Naâma, 45000, Algeria
[*]Corresponding author: e-mail: mousaab.beloudane@univ.usto.dz

The aim of this study is to investigate the effect of the blade shape on the characteristic of the flow patterns in a stirred tank. A new impeller blade design has been proposed. It is characterized by a converging hollow. The investigations of the flow structure generated in the vessel are made by using the computer code ANSYS CFX (version 16.0). The analysis has shown that the converging hollow blade yields highly radial flows which gave an increase in the radial velocity by 35% with less power consumption than the flat blade. Also, the effectiveness of the energy dissipation and the quality of mixing has been obviously noted. A validation test of our predicted results with other literature data was done, and a satisfactory agreement has been found.

Keywords: converging hollow, deep, radial flow, turbulent flow, stirred tank.

INTRODUCTION

The stirred tank has been used in a wide range of process application such as chemical, biochemical, food and pharmaceutical industries. The optimum design and the efficiency of mixing operations play the main role in product quality and production costs. Therefore, fundamental knowledge of velocity distribution and hydrodynamic behavior as well as power requirement of the stirred tank configuration is required. While the evolution of the stirred tanks have been done through the experimental technique which have many disadvantages such as cost and time, Computational Fluid Dynamics (CFD) techniques are being increasingly because these techniques provide the ultimate level of detail, less cost-effective and less time. The geometry of an impeller plays a paramount role in optimum design. For this purpose, various types of impellers are used in order to satisfy different of mixing operation.

A number of new impeller designs had been developed in order to improve the performance of conventional impeller (Rushton turbine). Hollow blade design is widely used in industry such as Concave blade, Chemineer CD-6 and SCABA SRGT, these have been respectively introduced by Van't Rietet al.[1], Bakker et al.[2] and Ni-enow[3].Indeed, many research efforts have been devoted to investigate effect of blade both by experimental and computational techniques. For example, Nagata studied experimentally the effect of the pitched blade on the power number with two pitched blades (PBT2). He found that this type of impeller requires less power consumption[4]. Suzukawa et al. studied the effect of the pitched blade in a baffled stirred tank equipped with a four pitched blade turbine (PBT4)[5]. Kumaresan and Joshi investigated the effect of the impeller blade angle, number of blades, blade width, blade twist, blade thickness, pumping direction on flow and turbulence field, with different impeller geometries. They found that the geometry of the blades can vary the fluid flow pattern and enhance the mixing intensity[6]. Driss et al. developed a computational method to study the effect of the pitched blade design on the stirred tank flow characteristics. Different inclined angles, equal to 45^0, $60^0$and 75^0 have been considered. The results show that the values of power number decreases as an inclined angles decreases with the same Reynolds number[7]. Ammar et al. studied numerically the effect of the impeller designs on the hydrodynamic structure induced by a three different turbines consisting on a six flat blades turbine, a Rushton turbine, a pitched blades turbine for the one-stage and two-stage systems. They concluded that the two Rushton turbines improve the circulation of the fluid in the whole volume of the tank[8]. Via Laser Doppler Velocimetry LDV technique, Aubin et al. studied the effect of the up-pumping and the down-pumping of a PBT turbine on the turbulent flow field and the power consumption as well as the pumping numbers. They deduced that the pumping upwards has a low flow number and consumes more power than the down-pumping[9]. Chapple et al. investigated the effect of the blade thickness and the impeller diameter on the power consumption,they found that changes in the impeller position can have a significant impact on the power number[10]. Ameur and Bouzit analysed numerically the effect of the impeller rotational speed, thefluid rheology and the impeller blade curvature on the mean velocities and power consumption. They found that the best performance is achieved at high Reynolds number for a flat-blade turbine,which requires more power consumption compared with the curved balde impeller[11]. By CFD method, Ameur and Bouzit investigated the effect of the impeller clearance, the blade diameter, the shape of the vessel base and the shape of the lower part of blade on the hydrodynamics behavior and shear rates distributions within the United States Pharmacopeia Apparatus[12]. Ameur et al investigated numerically the effect of some design parameters on the flow energy efficiency and the power consumption for a Maxblend impeller, an anchor impeller, a gate and double helical ribbon impellers. He found that the Maxblend impeller gives the best performance[13]. By CFD simulations, Khapre and Munshi carried out the numerical comparison of a Rushton Turbine and a CD-6 impeller and used the non-Newtonian fluid. They found that the flow field generated by a CD-6 impeller is less in magnitude than the Rushton turbine and the power consumption and entropy generation are less for CD-6

impeller[14]. By numerical simulations, Driss et al. confirmed that the multi-impellers systems can decrease the weak zones in each stirred tanks[15]. Ben Amira et al. studied experimentally via Particle image velocimetry (PIV) system effect of the blade turbine in the flow fields generated by an eight concave blades turbine. Moreover, they analysed experimentally with same technique the effect of up-pitching blade and they found that the velocity vector is directly affected by the turbine[16–17]. Cooke and Heggs found that the hollow blade turbines (HBT) designs are as energetically efficient as Rushton turbines for dispersing gas[18].

Basis of the previous studies, it is important to introduce new blade design that can provide the biggest advantage. Ghotli et al. analyzed via response surface methodology (RSM), the power requirements for seven types of 6-curved blade impellers of varying curvature angles and central disk sizes and compared to a Rushton turbine. They found that, the curved blade impellers have lower power consumption in both aerated and un-aerated conditions in comparison with the Rushton turbine[19]. Jing et al. used Particle image velocimetry technique for studied the effects of the blade shape on the trailing vortices in liquid flow agitated by four different disc impellers, including the Rushton type, concave blade disk impeller, half elliptical blade disk impeller, and parabolic blade disk impeller. The results showed that when the blade turns more curved, the inclination of the impeller stream becomes smaller and the radial jet becomes weaker[20].

For this purpose, the advanced Computational Fluid Dynamics (CFD) has been used in order to study flow pattern and power consumption. The major challenge is to develop a new blade design, that has the ability to improve flow fluid velocities. The purpose of this paper is to investigate the flow fields and the energy required for this type of impeller. We focus on the effect of new blade design. For this task, six geometrical blade configurations are used: a flat blade and five blades equipped with converging hollow with different deeps. Particularly, this paper presents the evolution of the velocity field and the turbulent characteristics on different planes, as well as the effect of this new blade design on the power consumption.

STIRRED TANK CONFIGURATION

The considered configuration consists of an unbaffled cylindrical tank with a flat bottom (Fig. 1). The liquid level H is equal to the diameter vessel D, with D = 490 mm. The impeller contains four flat-blade paddle, fixed on a disc with 20 mm of diameter which is attached to a cylindrical central shaft of diameter ds = 24.5 mm. The geometry system resembles that already studied by

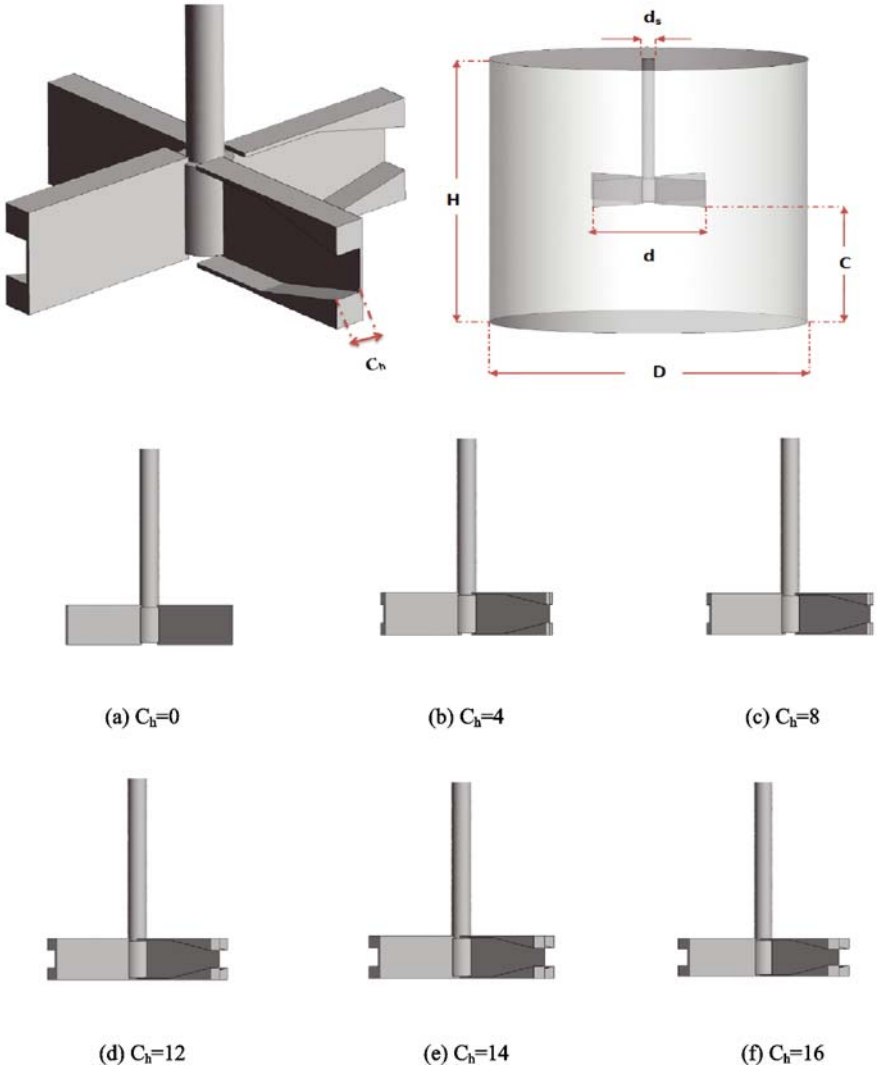

Figure 1. Geometrical arrangement

Nagata[4] as well as Suzukawa et al.[5] In order to investigate the effect of the converging hollow, four blade configurations are used: flat-blade with a height of 20 mm, and four blades equipped with converging hollow that have a different deep C_h = 4 mm, C_h = 8 mm, C_h = 12 mm, C_h = 14 and C_h = 16 mm. However, note that all of these impellers have the same blade perimeter h = 20 mm and the same diameter d = 245 mm and are placed at the same clearance from the tank bottom C = 245 mm.

NUMERICAL MODEL

Simulations are performed by using the computer code (CFX16.0). Since the stirred tank is not provided with baffles, a RRF (rotating reference frame) approach was used. In this approach, the tank was kept stationary while the vessel walls were assigned an angular velocity that was equal and opposite to the impeller rotational speed. The no-slip velocity condition was applied to all solid surfaces.

A pre-processor (ICEM CFD 16.0) is used to discretize the flow domain with a tetrahedral mesh (Fig. 2). Since the impeller has curved blades, an increased mesh density was generated near the impeller and vessel walls. The mesh density around the impeller was increased to accurately capture the blade design.

The original 3D mesh of the model had 150,258 computational cells. To verify the grid independency, the number of cells was increased from 153,258 cells to 306,516 cells. The additional cells changed the velocity magnitude in the regions of high velocity gradients by more than 3%. Thus, the number of cells was changed from 306,516 cells to 613,032 cells. The additional cells did not change the velocity magnitude in the regions of high velocity gradients and impeller power number by more than 2.5%. Therefore, 306,516 cells are employed in this study. The turbulent flow is defined (Reynolds number from 60000 to 100000).The second order upwind scheme is used for the convection terms. To perform pressure-velocity coupling, a pressure-correction method of the type Semi-Implicit Method for Pressure Linked Equations Consistent (SIMPLEC) is used. Solutions were converged when normalized residuals for pressure and velocity drop below 10^{-7}. Most calculations required 1000–1500 iterations and about 4–5 hours.

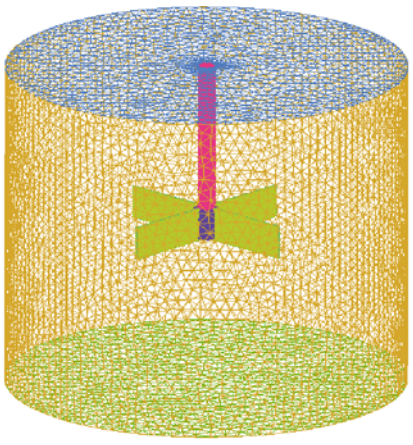

Figure 2. Meshing

Mathematical formulation

Total geometry of the mixing system is used as a computational domain (the quarter domain option was not employed). The using fluid is assumed incompressible and the corresponding flow equations are:

$$divV = 0 \tag{1}$$

$$\rho(VgradV + \omega(\omega r) + 2\omega V) + gradp - div\left[2\mu\left[\dot{\gamma}\right]\dot{\gamma}\right] = 0 \tag{2}$$

$\dot{\gamma} = \left(\frac{1}{2}\right)\left[gradV + \left(gradV\right)^{T}\right]$ is the rate of strain tensor, $\omega(\omega r)$ is the centrifugal acceleration, $2\omega V$ is the Coriolois acceleration, r is the radial coordinate and $\omega\left(\omega_x, \omega_y, \omega_z\right)$ is the angular velocity in clockwise direction.

For the boundary conditions,

– We impose at the vessel wall and bottom: $V = \omega r$ (3)

– On the impeller: $V = 0$ (4)

Further, the non-slip boundary condition is applied at the walls, and we have considered a closed tank in order to simulate the hydrodynamic structure of the stirred tank without considering the free surface motion. In our future paper, we intend to study the case of open stirred tanks.

Turbulent kinetic energy κ and the turbulent dissipation rate ε are calculated using RNG κ-ε turbulence model. This model was used by several authors such as Chtourou et al.[21], Jaworski and Zakrzewska[22].

Power number

The power number N_p allows to extrapolate calculations of the power when the diameter of the turbine d and its rotational speed N change. In dimensionless form, the power number is calculated in this numerical study by:

$$N_p = \frac{P}{\rho N^3 d^5} \tag{5}$$

P is the power consumption of the agitator system, given by:

$$P = 2\pi NS \tag{6}$$

Where, S is the torque of the agitator system.

The Reynolds number is written as follows:

$$R_e = \frac{\rho N d^2}{\mu} \tag{7}$$

All results are presented in dimensionless form:

$\varepsilon^* = \frac{\varepsilon}{N^3 d^2}$ dissipation rate of the turbulent kinetic energy (8)

$\kappa^* = \frac{\kappa}{N^2 d^2}$ turbulent kinetic energy (9)

RESULTS AND DISCUSSION

Comparison with experimental results

In order to check the validity of the CFD model and the used numerical method, a comparison is made between our predicted results and the experimental data given by Nagata[4]. The similar geometrical conditions are considered; also, the same fluid is simulated. Figure 3,

presents the predicted results for the radial velocity along the vessel height (Z/D) at a radial position (r/D = 0.5). According to these results, it has been noted that the gap between numerical results and those given by Nagata is about 5%. These results present a good agreement and confirm the validity of the numerical method.

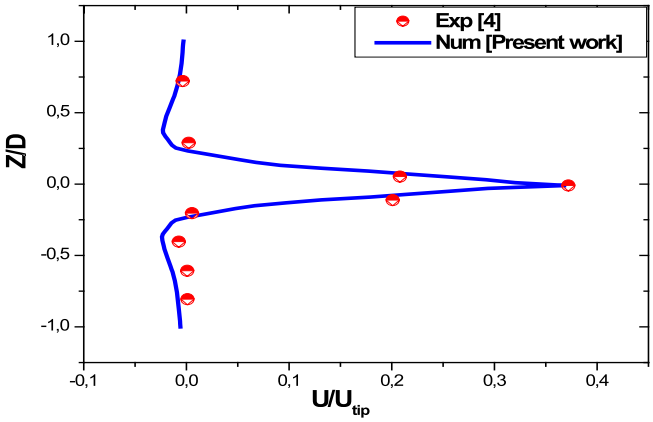

Figure 3. Axial profile of the radial velocity, Re = 100000, θ = 0^0

Radial velocity

In this paper, the effects of the converging hollow assembled on the blade have been investigated. In order to understand the effect of blade shape on the flow characteristics, the variation of the radial velocity component along the vessel height for different converging hollow assembled to the blade are plotted in Figure 4, for a radial position near the blade tip r/D = 0.5 and

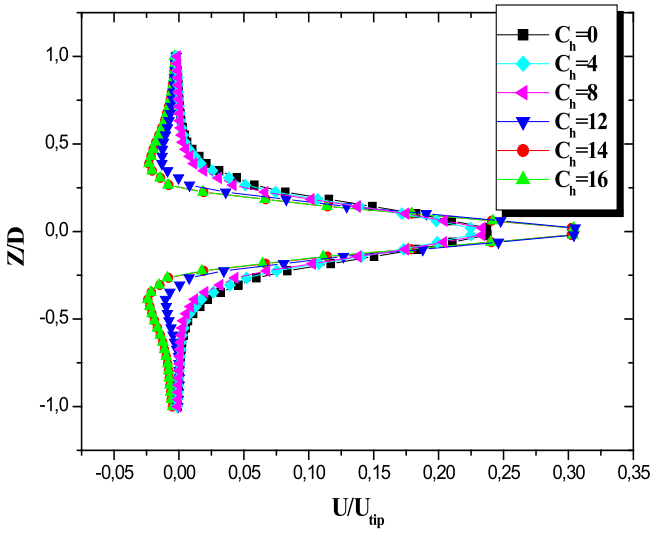

Figure 4. Radial velocity profiles for different C_h, in the r-z plane, defined by Re = 60000, θ = 0^0, r/D = 0.5

Re = 60000 the angular coordinate is equal to θ = 0°. The negative values of the radial component prove the existence of the recirculation loop just above and below the turbine, and it vanishes in the top and bottom of the tank in all blade configurations. By comparing the different configurations an increase of the radial component of the magnitude velocity with 35% for the blade configuration defined by C_h = 12. On the other hand, it's noticeable that C_h = 12, 14, 16 generate the same radial velocity. The explanation of this increase is that the new blade design dissipates less energy than the standard blade.

As presented in Figure 5 for Re = 100000 it has been observed that the impeller stream flows away from the

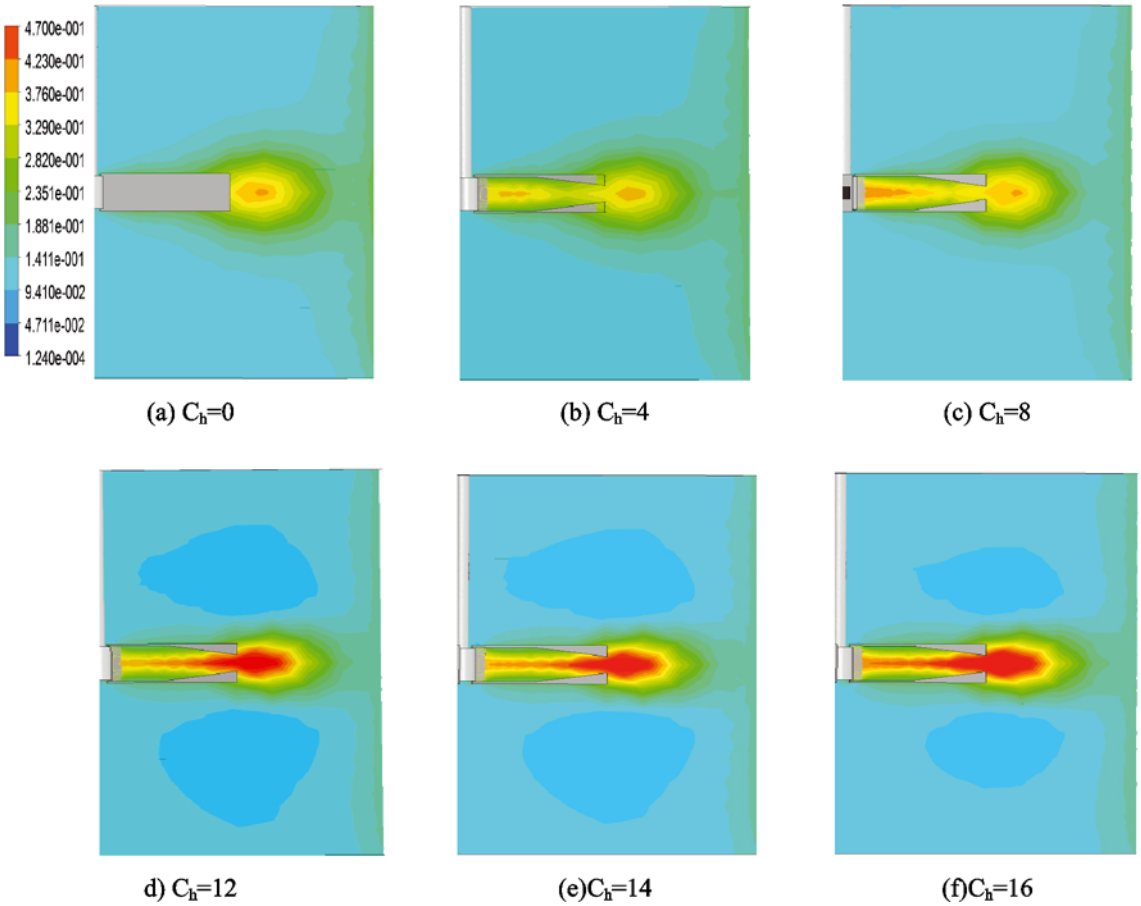

Figure 5. Distribution of the dimensionless radial velocity, in the r-z plane defined by Re =100000, θ = 0^0

impeller blades, and the velocity varies dramatically in the radial direction. Therefore, we can deduce that the new configuration of blade plays an important role on the variation of radial velocity. The movement of fluid becomes more intense in the radial velocity with increasing deep of converging hollow. Indeed, the radial velocity is stronger with converging hollow configuration.

Tangential velocity

The variations of the tangential velocity component along the vessel radius and for the six cases studied are plotted in Figure 6, at the mid height of the impeller blade. According to these results, the intensity of the flow marks at the tips of the blade. This intensity is lost near to the side walls of the tank. After that, it becomes negligible at the immediate contact with the wall. Indeed, it has been observed that curve decay is faster with the converging hollow $C_h = 12$, $C_h = 14$ and $C_h = 16$. From these results, it could be deduced that the new blade configuration affect the tangential velocity that decreases as soon as the depth of the converging hollow increase.

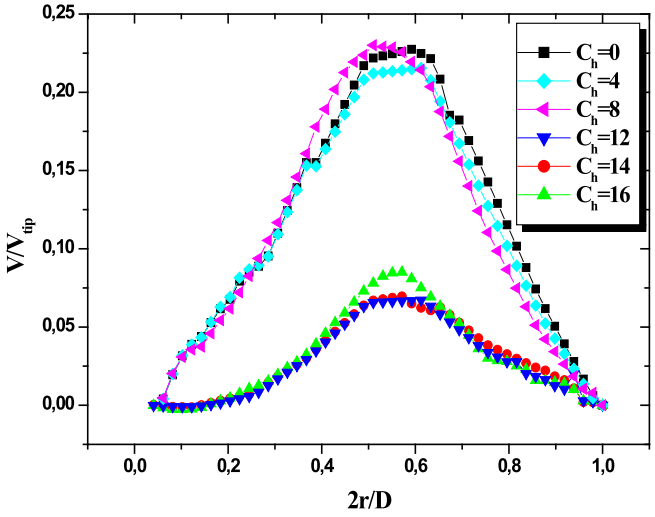

Figure 6. Profile of tangential velocity for C_h

Axial velocity

Figure 7 presents the axial velocity profile along the vessel height (Z/D) for a radial position near to the blade tip. According to these results, it has been observed that the axial velocity component was the highest value in the area swept by the impeller. The low value of the axial velocity component indicates the apparition of the recirculation zone. Compared with the flat blade, it can be seen that new blade configuration has a few effect on the axial component of the mean velocity. Therefore, we can deduce that the increase of C_h has no effect of the axial flow.

Mean velocity

Figure 8 shows the distribution of the mean velocity at various blade configurations for the angular position $\theta = 45^o$. Globally, it has been noted that the appearance of the maximum values developed in the area swept by the turbine. Moreover, we find that the flat-blade generates a larger swept surface that gives wider cavern than other blade configuration.

According to these results, it can be concluded that the new impeller design enhance only the radial flow.

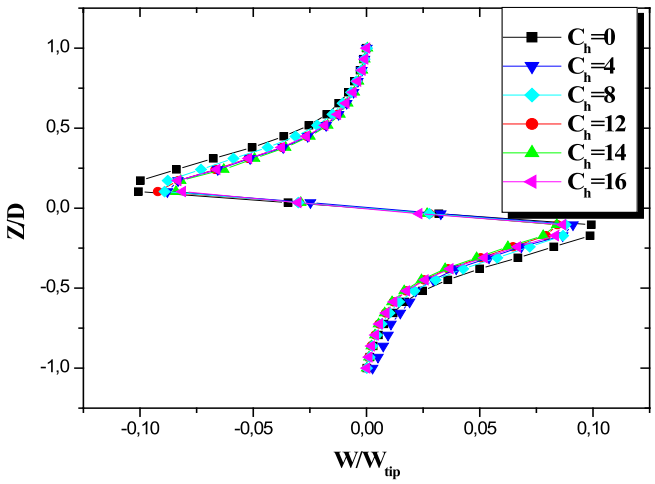

Figure 7. Axial velocity for different C_h

Velocity streamlines

Figure 9 presents the streamlines velocity in 3D view. According to these results, a significant change in streamline behavior is shown by changing the system from flat blade to converging hollow configuration. Particularly, it has been observed that the flow is disturbed and created a complicated flow field with further increase of the deep of converging hollow. For more significant C_h, the outgoing flow from the blades becomes larger which improve the mixing quality throughout the vessel.

Turbulent kinetic energy

The turbulent kinetic energy has a significant impact on the performance of a stirred tank. The distribution of the turbulent kinetic energy in the r-z plane containing the turbine for a position corresponding to the angular coordinate $\theta = 45^o$ for different blade configurations is shown in Figure 10. We found three studied zones: the discharge zone, the upper zone and the lower zone. The turbulent kinetic energy is maximum in the discharge zone. It increases in the area swept by the impeller that proves the existence of good mixing in this area. Indeed, numerical simulation shows that a new impeller design exhibits higher turbulent kinetic energy than standard impeller due to the significant radial jet generated by this type of the blade.

Dissipation rate of the turbulent kinetic energy

Figure 11 presents the distribution of the dissipation rate of the turbulent kinetic energy in the horizontal plane situated in the middle of the blade. Globally, it has been noted that the dissipation rate of the turbulent kinetic energy is concentrated in the area swept by the turbine. Beyond this zone, it decreases gradually. Indeed, the shape of the wake depends on the discharge jet of the turbine. This fact explains that the new blade designs have a direct effect on the dissipation rate of the turbulent kinetic energy.

Power consumption

The power consumption is the important parameter for describing the mixing efficiency. Here, Figure 12 presents the variation of the power consumption required for different converging hollow. According to these results, power number decreases continuously with the increase in the deep of converging hollow. Based on the

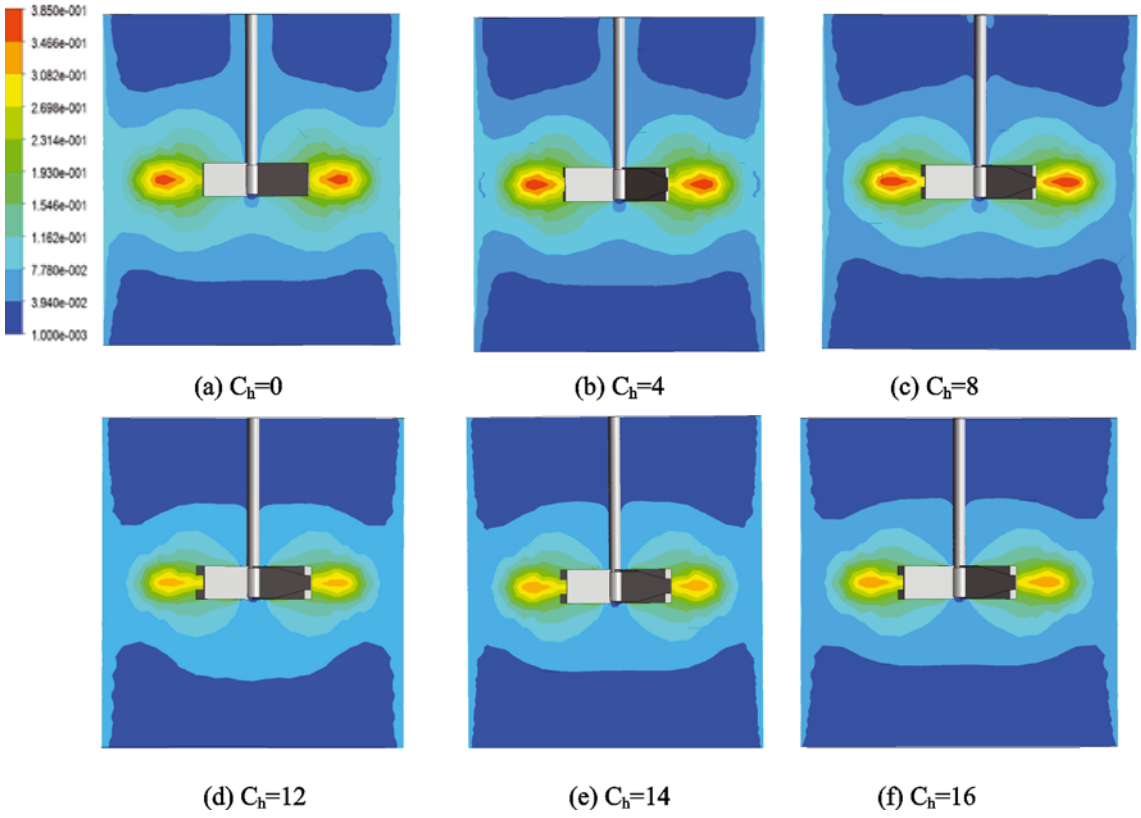

Figure 8. Distribution of mean velocity for different Ch at the angular position $\theta = 45^0$

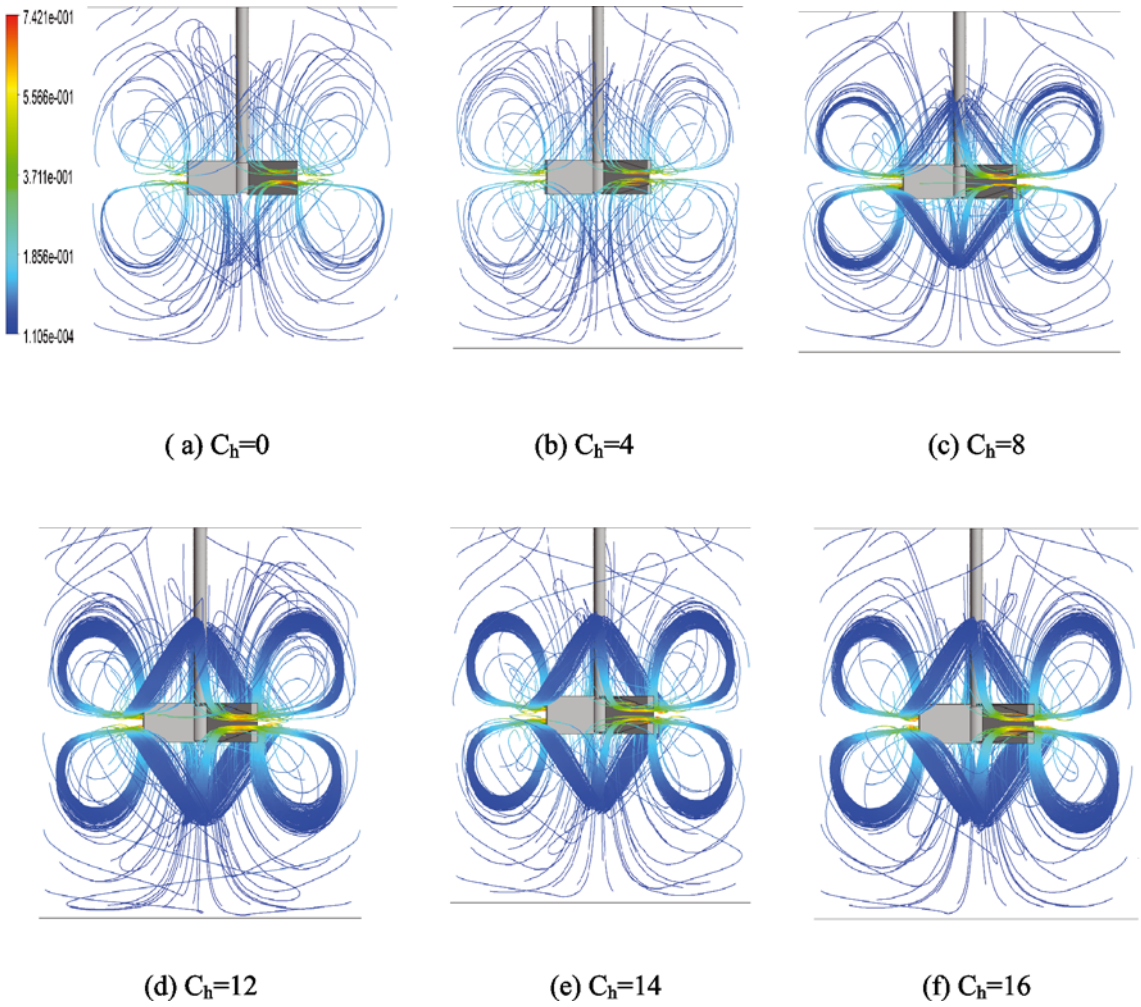

Figure 9. Streamline for different C_h (3D)

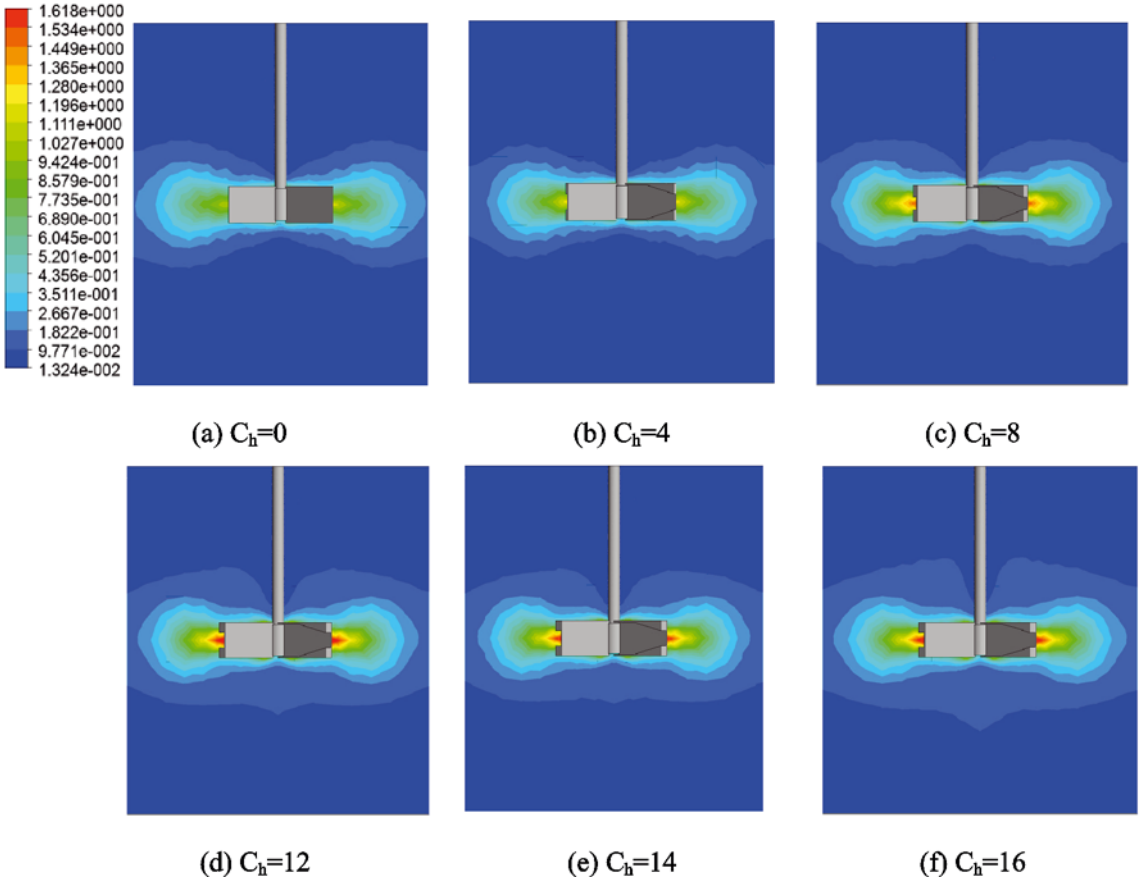

Figure 10. Distribution of Turbulent kinetic energy κ^* for different C_h, in the angular position $\theta = 45^0$

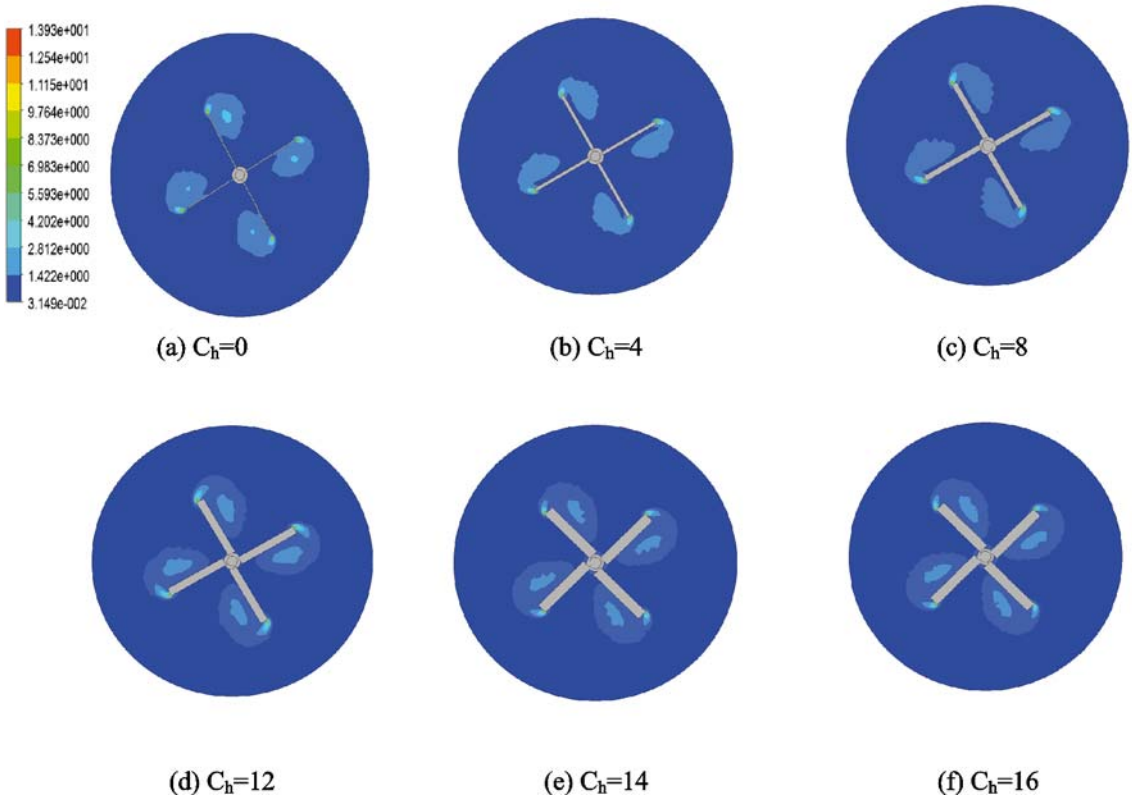

Figure 11. Distribution of the dissipation rate of the turbulent kinetic energy ε^* for different C_h, in r-θ plane

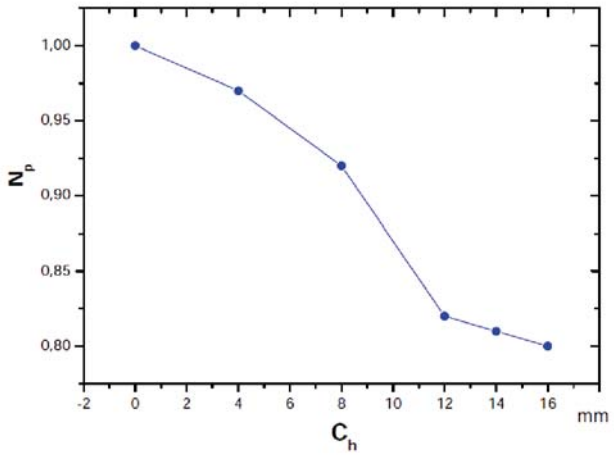

Figure 12. Power number for different C_h

finding results and in order to reduce the mixing power, it is recommended to use this new blade configuration.

CONCLUSION

In this work, we have studied the effect of the new blade design on the hydrodynamic structure in the turbulent flow generated in the stirred vessels. Based on above results, the following conclusions are drawn:

The new impeller design gave an increase in radial velocity by 35%.

A new impeller design exhibits higher turbulent kinetic energy than standard impeller due to the significant radial jet generated by this type of blade.

The values of the power number decrease when deep converging hollow increases at the same Reynolds number.

CFD models can be used to realize and test the effectiveness of new blade design.

Results showed also that the outgoing flow from the blades is more active with the new design impeller. In this case, the effectiveness of mixing quality has been obviously noted.

NOMENCLATURE

C – impeller clearance, (m)
C_h – deep of converging hollow, (mm)
D – tank diameter, (m)
d – impeller diameter, (m)
d_s – shaft diameter, (m)
H – height of the tank, (m)
κ – turbulent kinetic energy, ($m^2 \cdot s^{-2}$)
κ' – turbulent kinetic energy, dimensionless
N – rotating speed of the impeller, (s^{-1})
N_p – power number, dimensionless
P – power, (W)
p – pressure, (Pa)
r – radial coordinate,(m)
$2r/D$ – dimensionless radial coordinate
R_e – Reynolds number, dimensionless
S – torque of the agitator system,(N.m)
t – time, (s)
Z – axial coordinate, (m)
U/U_{tip} – radial velocity component, dimensionless
V/V_{tip} – tangential velocity components, dimensionless
V – velocity, ($m \cdot s^{-1}$)
W/W_{tip} – axial velocity component, dimensionless

Greek Letters

θ – angular coordinate, degree
ω – angular velocity, ($rad \cdot S^{-1}$)
ρ – density of fluid, ($kg \cdot m^{-3}$)
μ – dynamic viscosity of the fluid, ($Pa \cdot s$)
ε – dissipation rate of the turbulent kinetic energy, ($m^2.s^{-3}$)
ε^* – dissipation rate of the turbulent kinetic energy, dimensionless

LITERATURE CITED

1. Van't riet, K., Boom, J.M. & Smith. J.M. (1976). Power consumption impeller coalescence and recirculation in aerated vessels. *Trans. I. Chem E*. 541, 124–131.

2. Bakker, A., Myers, K.J. & Smith, J.M (1994). How to disperse gases in liquids. *Chemical Engineering*. 101, 98–104, from http://www.bakker.org/cfm/publications/HowtoDisperse-GasesinLiquids1994.pdf

3. Nienow, A.W. (1996). Gas-Liquid Mixing Studies, A comparison of Rushton Turbines with some modern impellers. *Trans. I. Chem. E.* 74 A, 417–423. DOI: 10.1002/cjce.5450800409.

4. Nagata, S. (1975). Mixing Principals and Applications. John Wiley & sons Halstead Press Tokyo Japan.

5. Suzukawa, K., Mochizukib, S. & Osaka, H. (2006). Effect of the attack angle on the roll and trailing vortex structures in an agitated vessel with a paddle impeller. *Chem. Engineer. Sci.* 61, 2791–2798. DOI: http://dx.doi.org/10.1016/j.ces.2005.10.063.

6. Kumaresan, T. & Joshi, J.B. (2006). Effect of impeller design on the flow pattern and mixing in stirred tanks. *Chem. Eng. Sci*. 1153, 173–193. DOI: 10.1016/j.cej.2005.10.002.

7. Driss, Z., Bouzgarrou, G., Chtourou, W., Kchaou, H. & Abid, M.S. (2010). Computational studies of the pitched blade turbines design effect on the stirred tank flow characteristics. *European J. Mechanics B/Fluids*. 29, 236–245. DOI: 10.1016/j.euromechflu.2010.01.006.

8. Ammar, M., Chtourou, W., Driss, Z. & Abid, M.S. (2011). Numerical investigation of turbulent flow generated in baffled stirred vessels equipped with three different turbines in one and two-stage system. *Energy*, 36, 5081–5093. DOI: http://dx.doi.org/10.1016/j.energy.2011.06.002.

9. Aubin, J., P. Mavros, D. Fletcher, J. & Bertrand C. Xuereb. (2001) .Effect of axial agitator configuration up-pumping down-pumping reverse rotation on flow patterns generated in stirred vessels. *Chem. Engineer. Res. Design.* 79, 845–856. DOI: 10.1205/02638760152721046.

10. Chapple, D., S. kresta, Wall, A. & Afcan, A. (2002). The effect of Impeller and Tank Geometry on Power Number for a pitched blade turbine. *Chem. Engineer. Res. Design*. 804, 364–372. DOI: http://dx.doi.org/10.1205/026387602317446407

11. Ameur, H. & Bouzit, M. (2013) .Numerical investigation of flow induced by a disc turbine in unbaffled stirred tank. *Acta Sci. Tech.* 35, 469–476. DOI: http://dx.doi.org/10.4025/actascitechnol.v35i3.15554

12. Ameur, H. & Bouzit, M. (2013). 3D hydrodynamics and shear rates variability in the united states pharmacopeia paddle dissolution apparatus. *Int. J. Pharm.* 452, 42−51. DOI: 10.1016/j.ijpharm.2013.04.049

13. Ameur, H. (2015) .Energy efficiency of different impellers in stirred tank reactors. *Energy*. 93, 1980–1988. DOI: doi.org/10.1016/j.energy.2015.10.084.

14. Khapre, A. & Munshi, B. (2014) .Numerical Comparison of Rushton Turbine and CD-6 Impeller in Non-Newtonian Fluid Stirred Tank. International Scholarly and Scientific Research & Innovation. 811, 1235–1242. Available at: scholar.waset.org/1999.2/5555526.

15. Driss, Z., Karray, S., Chtourou, W., Kchaou, H. & Abid, M.S (2012).A study of mixing structure in stirred tanks

equipped with multiple four-blade Rushton impellers., *The Archive of Mechanical Engineering*. 591, 53–72. DOI: https://doi.org/10.2478/v10180-012-0004-3.

16. Ben Amira, B., Driss, Z. & Abid, M.S. (2015). PIV study of the turbulent flow in a stirred vessel equipped by an eight concave blades turbine. *Fluid Mechanics*. 12, 5–10. DOI: 10.11648/j.fm.20150102.11.

17. Ben Amira, B., Driss, Z. & Abid, M.S. (2015).Experimental study of the up-pitching blade effect with a PIV application. *Ocean Engineer.* 102, 95–104. DOI: 10.1016/j.oceaneng.2015.08.063.

18. Cooke, M. & Heggs, P.J. (2005). Advantages of the hollow (concave) turbine for multi-phase agitation under intense operating conditions. *Chem. Engineer. Sci*. 60, 5529–5543. DOI: https://doi.org/10.1016/j.ces.2005.05.018

19. Ghotli, R.A., Abdul, Aziz A.R., Ibrahim, S., Baroutian, S. & Arami-Niya, A. (2013). Study of various curved-blade impeller geometries on power consumption in stirred vessel using response surface methodology. *J. Taiwan Inst. Chem. Eng*.44, 192–201. DOI: http://dx.doi.org/10.1016/j.jtice.2012.10.010

20. Jing, Z., Zhengming, G. & Yuyun, B., (2011). Effects of the Blade Shape on the Trailing Vortices in Liquid Flow Generated by Disc Turbines. *Chinese J. Chem. Engineer*. 19(2), 232–242. DOI: 10.1016/S1004-9541(11)60160-2.

21. Chtourou, W., Ammar, M., Driss, Z. & Abid, M.S. (2011). Effect of the turbulence models on Rushton turbine generated flow in a stirred vessel. *Cent. Eur. J. Eng*. 1(4), 380–389. DOI: 10.2478/s13531-011-0039-0.

22. Jaworski, Z. & Zakrzewska, B. (2002). Modeling of the turbulent wall jet generated by a pitched blade turbine impeller. *Trans Ichem. E*. 80(8), 846–854. DOI: http://dx.doi.org/10.1205/026387602321143381.